Chemically-Induced Cell Wall Stapling in Bacteria

Sylvia L. Rivera[1,9], Akbar Espaillat[2,9], Arjun K. Aditham[3,4,9], Peyton Shieh[5], Chris Muriel-Mundo[1], Justin Kim[6,7], Felipe Cava[2,*], M. Sloan Siegrist[1,8,10,*]

[1]Department of Microbiology, University of Massachusetts, Amherst, MA 01003, USA

[2]Laboratory for Molecular Infection Medicine, Department of Molecular Biology, Umeå University, Umeå 90187, Sweden

[3]Department of Bioengineering, Stanford University, Stanford, CA 94305, USA

[4]Stanford ChEM-H (Chemistry, Engineering, and Medicine for Human Health), Stanford University, Stanford, CA 94305, USA

[5]Department of Chemistry, Massachusetts Institute of Technology, 77 Massachusetts Avenue, Cambridge, MA 02139, USA

[6]Department of Cancer Biology, Dana-Farber Cancer Institute, Boston, MA 02215, USA

[7]Department of Biological Chemistry and Molecular Pharmacology, Harvard Medical School, Boston, Massachusetts 02115, USA

[8]Molecular and Cellular Biology Program, University of Massachusetts, Amherst, MA 01003, USA

[9]These authors contributed equally

[10]Lead contact

[*]Correspondence: siegrist@umass.edu (M.S.S), felipe.cava@umu.se (F.C.)

Summary

Transpeptidation reinforces the structure of cell wall peptidoglycan, an extracellular heteropolymer that protects bacteria from osmotic lysis. The clinical success of transpeptidase-inhibiting β-lactam antibiotics illustrates the essentiality of these cross-linkages for cell wall integrity, but the presence of multiple, seemingly redundant transpeptidases in many bacterial species makes it challenging to determine cross-link function. Here we present a technique to covalently link peptide strands by chemical rather than enzymatic reaction. We employ bio-compatible click chemistry to induce triazole formation between azido- and alkynyl-D-alanine residues that are metabolically installed in the cell walls of Gram-positive and Gram-negative bacteria. Synthetic triazole cross-links can be visualized by substituting azido-D-alanine with azidocoumarin-D-alanine, an amino acid derivative that undergoes fluorescent enhancement upon reaction with terminal alkynes. Cell wall stapling protects *Escherichia coli* from β-lactam treatment. Chemical control of cell wall structure in live bacteria can provide functional insights that are orthogonal to those obtained by genetics.

Introduction

Cell wall peptidoglycan is a mesh-like biopolymer that surrounds nearly all bacteria and is required to resist turgor pressure. The macromolecule consists of a glycan backbone and peptides, containing both L- and D-amino acids (Figure 1A), that

are cross-linked by D,D- and L,D-transpeptidases (Egan et al., 2015). The degree of transpeptidation can vary with species, growth phase and environmental conditions (Vollmer and Seligman, 2010). For example, the peptidoglycan of slow- or non-growing *E. coli* is more highly cross-linked and less susceptible to *in vitro* enzymatic turnover than that of actively-replicating *E. coli* (Glauner et al., 1988; Goodell and Tomasz, 1980; Lee et al., 2013; Pisabarro et al., 1985; Tuomanen and Cozens, 1987; Tuomanen et al., 1988). Cross-linking abundance is also predicted to impact the overall strength and stiffness of the cell envelope (Auer and Weibel, 2017; Huang et al., 2008; Loskill et al., 2014; Vollmer and Bertsche, 2008), cell shape (Huang et al., 2008; Sycuro et al., 2010; Yang et al., 2019), and assembly of macromolecular structures (Scheurwater and Burrows, 2011). The clinical success of transpeptidase-inhibiting β-lactam antibiotics highlights the importance of peptidoglycan cross-linking in bacterial physiology.

Despite the biological and medical significance of peptidoglycan transpeptidation, unraveling the roles of these linkages is challenging. Currently, the standard ways to manipulate cross-linking are to mutate or deplete the expression of the transpeptidase genes or to inhibit these enzymes with small molecules like β-lactams. However, the functional redundancy of transpeptidases and promiscuity of β-lactams (Spratt, 1975) pose challenges to rational control of peptidoglycan connectivity.

D-amino acids bearing reactive groups such as cysteines, alkynes, azides and tetrazines have been used to metabolically label the peptidoglycan stem peptide (de Pedro et al., 1997; Kuru et al., 2012; Pidgeon et al., 2015; Radkov et al., 2018; Siegrist

et al., 2015; Siegrist et al., 2013). Once embedded, the presence of these probes can be revealed by chemical reaction with an exogenous label that bears a complementary reactive group (Siegrist et al., 2015). We hypothesized that we might also use functionalized peptide strands to manipulate cell wall cross-linking. More specifically, we reasoned that co-incubation of bacteria with azido- and alkynyl-D-amino acids would result in a subpopulation of labeled muropeptide strands in close enough proximity to undergo copper-catalyzed azide-alkyne cycloaddition (CuAAC) upon introduction of the appropriate reagents (Figure 1B). Such structures would serve as synthetic, triazole cross-links.

Results and Discussion

We first tested our hypothesis using a loss-of-fluorescence assay. In this approach, bacteria are co-incubated in the presence of azido- and alkynyl-D-amino acids, washed and subjected to CuAAC (Figure 2A, left). We reasoned that the peptidoglycan-embedded functional groups should either react with each other or with the alkynyl- or azido-fluorophores in CuAAC solution. Bacteria incubated with a single D-amino acid probe, by contrast, should have muropeptides decorated with just one functional group, which in turn should react only with the complementary reactive fluorophore. In this assay, we interpret decreased labeling of co-incubated relative to singly-incubated bacteria to indicate that there are fewer peptidoglycan-embedded functional groups available to react with the fluorophores. This may occur because the reaction between azido- and alkynyl-muropeptides is favored or because there is

competition between the D-amino acids for initial incorporation into the muropeptide. To control for the latter possibility, we also subjected metabolically-labeled bacteria to strain-promoted azide-alkyne cycloaddition (SPAAC; Figure 2A, right) with a cyclooctyne-appended fluorophore. In the absence of copper and other reagents, peptidoglycan-embedded azides and alkynes should not react with each other at an appreciable rate and only the azide-cyclooctyne reaction should occur. In the SPAAC reactions, therefore, we interpret changes in labeling to mean that the azido-D-amino acid outcompetes or is outcompeted by other D-amino acids for initial incorporation into the cell wall.

We used the loss-of-fluorescence approach to ask whether we could introduce triazole cross-links into the cell wall of *Listeria monocytogenes*, a Gram-positive, food-borne pathogen. We initially used *pbp5::tn L. monocytogenes*, a D,D-carboxypeptidase-deficient mutant that we previously showed has high levels of D-amino acid labeling (Siegrist et al., 2013). After incubating the bacteria in the presence of equal amounts of D-alanine (Dala), azido-D-amino acid (azDA or azDlys, the R groups of which respectively have one and four carbons), alkynyl-D-alanine (alkDA) or mixtures thereof, we washed away unincorporated amino acid and subjected the bacteria to CuAAC with either an alkynyl- (Figure 2B) or azido-fluorophore (Figure 2C). We assessed cellular fluorescence by flow cytometry. In both cases, the bacteria that were co-incubated in alkDA/azDlys had lower amounts of fluorescence than those incubated in azDlys (Figure 2B) or alkDA (Figure 2C) alone. We obtained similar results with the more bio-friendly CuAAC reaction (Yang et al., 2014) that employs the 3-[4-({bis[(1-tert-butyl-1H-

1,2,3-triazol-4-yl)methyl]amino}methyl)-1H-1,2,3-triazol-1-yl]propanol (BTTP) ligand (Wang et al., 2011) (Figure 2D) or in wild-type *L. monocytogenes* (Figures S1A and S1B). These data suggested that bacteria co-incubated in azDlys and alkDA had fewer peptidoglycan-embedded functional groups available to react with complementary reactive fluorophores in solution (Figure 2A). Moreover, in bacteria subjected to SPAAC with cyclooctyne-fluorophore, the signal after alkDA/azDlys incubation was similar to that of azDlys alone or Dala/azDlys (Figures 2E and S1C). The SPAAC control reactions suggested that there was no appreciable competition between the D-amino acids for initial incorporation into the peptidoglycan. Taken together these data suggest that cell wall-embedded azides and alkynes can react with each other by CuAAC.

We next sought a more direct read-out for triazole cross-links. Fluorogenic molecules undergo a fluorescence enhancement upon chemical or enzymatic reaction. For example, CuAAC reaction of the non-fluorescent 3-azido-7-hydroxycoumarin (azido-coumarin) with terminal alkynes yields fluorescent triazole products (Sivakumar et al., 2004). As D-amino acids appended to fluorophores, including hydroxycoumarin, incorporate efficiently into peptidoglycan (Kuru et al., 2012), we decided to test whether swapping an azido-coumarin D-amino acid (azcDA) for an azido-D-amino acid would allow us to mark the presence of triazole cross-links (Figure 2F).

We began by synthesizing azcDA, which could be accessed readily by coupling N^{α}-Boc-D-2,3-diaminopropionic acid to azidocoumarin acid **1** (Weineisen et al., 2017) via pentafluorophenyl ester **2**. Trifluoroacetic acid-mediated Boc deprotection afforded

azcDA (Scheme 1). Next we co-incubated *pbp5::tn L. monocytogenes* with Dala/azcDA or alkDala/azcDA, washed, and subjected the bacteria or not to a BTTP CuAAC reaction that lacked a complementary alkynyl-fluorophore. By microscopy we found that fluorescence of live, azcDA-labeled bacteria required the inclusion of alkDA in the initial metabolic labeling step as well as the subsequent CuAAC reaction (Figure 2G). These gain-of-fluorescence data were consistent with the loss-of-fluorescence results (Figures 2B-2D, S1A, S1B) and supported the notion that a CuAAC reaction can covalently join azides and alkynes metabolically installed in *L. monocytogenes* peptidoglycan to form synthetic cross-links.

We were initially unable to identify peptidoglycan modifications that were specific to alkDA/azDlys-treated, CuAAC-subjected bacteria and that had the exact mass of a triazole cross-link (Figure S2). We hypothesized that our ability to detect such modifications—which theoretically could include muropeptides with additional, transpeptidase-mediated linkages—was complicated by the pre-existing complexity of *L. monocytogenes* peptidoglycan, which is both highly-cross-linked and tailored by *N*-deacetylases, *O*-acetyltransferases and amidotransferases (Aubry et al., 2011; Boneca et al., 2007; Rae et al., 2011). Therefore, we turned our attention to the model, Gram-negative bacterium *Escherichia coli*, as its peptidoglycan composition is considerably less complex (Vollmer et al., 2008). To simplify our analysis even more, we employed a strain, CS802-2, in which most of the genes encoding peptide-acting cell wall enzymes were deleted, including all 6 carboxypeptidases (Denome et al., 1999). The lack of tetrapeptides in this background prevents L,D-transpeptidation, so we expected D-amino

158 acid incorporation to occur at the 5th position of the stem peptide (Cava et al., 2011). We
159 first verified that CuAAC-subjected, alkDA/azDA-labeled CS802-2 *E. coli*, like wild-type
160 *E. coli*, were less fluorescent than those labeled by azDA or alkDA alone (Figures 3A,
161 3B, S3) The decrease in D-amino acid concentration and labeling time compared to *L.*
162 *monocytogenes* (described further below) correlated with a more modest reduction in
163 fluorescence. We next metabolically labeled CS802-2 *E. coli* with different combinations
164 of D-amino acids, washed away unincorporated amino acid, and performed BTTP
165 CuAAC reactions in the absence of fluorophore. We then separated digested
166 peptidoglycan by ultra-performance liquid chromatography (UPLC) and used MS/MS to
167 identify molecules with the exact masses that corresponded to azDA- and alkDA-
168 terminating pentapeptides in the appropriate samples. We identified peaks that were
169 specific to alkDA/azDA-treated, CuAAC-subjected bacteria (Figure 3C) and had the
170 exact masses of a 5-5 triazole dimer, trimer (+/- anh) or tetramer (Figures 3D-E, S4, S5,
171 and Table S1). The presence of these species increased the total cross-linking by
172 approximately 20% (Table 1). We note that muropeptide incorporation of azDA was ~2-
173 fold more efficient than alkDA and associated with a general decrease in cross-linking
174 (Tables 1 and S2). Exogenous D-amino acids, including both Dala and non-canonical D-
175 amino acids, have been shown or hypothesized to inhibit D,D-transpeptidation (Caparros
176 et al., 1992; Lam et al., 2009). Importantly, however, CuAAC-dependent cross-linking
177 occurred only in alkDA/azDA-treated samples (Table 1) and not in controls that had
178 been treated with equimolar amounts of Dala/azDA (Table S2) or Dala alone (Table 1).
179 These data confirmed our ability to introduce synthetic cross-links into bacterial
180 peptidoglycan in a CuAAC-inducible manner.

Cell wall homeostasis is a balance between synthesis and turnover. Peptidoglycan-cleaving enzymes have been implicated directly (Park and Strominger, 1957; Schwarz et al., 1969; Tomasz et al., 1970; Tomasz and Waks, 1975) and indirectly (Cho et al., 2014; Kohlrausch and Höltje, 1991) in β-lactam cidality. Slow- or non-replicating, β-lactam-tolerant *E. coli* have highly cross-linked cell walls that are more resistant *in vitro* to lytic enzymes (Glauner et al., 1988; Goodell and Tomasz, 1980; Lee et al., 2013; Pisabarro et al., 1985; Tuomanen and Cozens, 1987; Tuomanen et al., 1988). We wondered whether β-lactam susceptibility might be influenced by pre-existing cell wall cross-linking, either in addition to, or as part of, the well-documented effect of bacterial growth rate (Eng et al., 1991; Lee et al., 2018; Lee et al., 1944; Toumanem et al., 1986). Since exogenous D-amino acids can modify the structure, amount and strength of peptidoglycan and inhibit bacterial growth (Caparros et al., 1992; Cava et al., 2011; Lam et al., 2009), and growth rate in turn correlates with β-lactam lethality (Eng et al., 1991; Lee et al., 2018; Lee et al., 1944; Toumanem et al., 1986), we first optimized D-amino acid concentration and incubation time (Figures S6A and S6B). We then labeled *E. coli* with different combinations of D-amino acids, washed and performed BTTP CuAAC. After CuAAC reagent washout, bacteria were resuspended in growth medium and challenged with the β-lactam ampicillin. Without CuAAC, ampicillin treatment resulted in similar killing regardless of what D-amino acid(s) the bacteria had been metabolically labeled with (Figure 4A). In *E. coli* subjected to CuAAC, ampicillin caused ~2-3 logs of killing for bacteria labeled with Dala, Dala/alkDA

or Dala/azDA but less than 1 log for those labeled with alkDA/azDA (Figure 4B). These data suggested that triazole cross-links protect *E. coli* from ampicillin.

BTTP-liganded CuAAC (Wang et al., 2011) is more biocompatible than traditional TBTA CuAAC (Yang et al., 2014). While the BTTP CuAAC reaction that we previously optimized for mycobacterial species (Garcia-Heredia et al., 2018) did not change *L. monocytogenes* cell counts (Figure S7), they partially inhibited the recovery of *E. coli* on solid medium (Figure 4). However the effect was consistent across the different D-amino acid combinations, indicating that the synthetic cross-links, not the CuAAC, were responsible for antibiotic rescue. In liquid medium, *E. coli* subjected to CuAAC had a distinct lag in growth relative to mock-reacted controls (Figures S6C-S6E). The length of the lag phase was significantly enhanced in CS802-2 *E. coli* that had been incubated in both azDA and alkDA *e.g.* bacteria with triazole linkages. Since longer lag phases are associated with antibiotic tolerance (Bertrand, 2019; Fridman et al., 2014) we asked whether the apparent protection afforded by alkDA/azDA labeling followed by CuAAC was transient and whether it was specific to β-lactams. During the post-CuAAC lag phase, synthetic cross-links protected bacteria from ampicillin and the closely-related antibiotic carbenicillin (Figures 4B, S7A, S7B) but not the translation-inhibiting aminoglycoside kanamycin (Figure 4C). This protection was lost following resumption of growth (Figure S7C). Thus an extended, post-CuAAC lag phase correlates with, but is likely not responsible for, the enhanced tolerance of alkDA/azDA-labeled *E. coli* to β-lactams.

Taken together, our data suggest that synthetic peptidoglycan cross-links protect against β-lactam-induced lethality. The total cross-linking density across CuAAC-treated bacteria is similar (Tables 1 and S2), suggesting that the unusual linkage (triazole) or position on the stem peptide (5-5) is instead responsible for protection. The classic view of β-lactam activity is that transpeptidase inhibition damages the cell wall by disrupting the balance between peptidoglycan synthases and hydrolases (Park and Strominger, 1957; Schwarz et al., 1969; Tomasz et al., 1970; Tomasz and Waks, 1975). β-lactams also induce a metabolically-taxing, futile cycle of cell wall synthesis and turnover (Cho et al., 2014; Kohlrausch and Höltje, 1991). Both models for β-lactam cidality posit that lethality directly or indirectly depends on the activity of peptidoglycan-degrading enzymes. An artificially-reinforced cell wall may resist β-lactam-induced damage because its structure is partially independent from transpeptidase-mediated synthesis. Additionally, or alternatively, synthetic cross-links may regulate peptidoglycan turnover. Indeed, while this manuscript was under review, Dik and colleagues proposed that non-canonical cell wall cross-links (derived from the reaction of exogenously-incorporated sulfonyl fluoride D-amino acids with endogenous *m*-DAP) can impede the processivity of lytic transglycosylases (Dik et al., 2020), enzymes that cleave the carbohydrate backbone of peptidoglycan. While we cannot rule out pleiotropic effects on other cell envelope or periplasmic structures, we hypothesize that synthetic triazole cross-links act as molecular speed bumps for lytic transglycosylases, blunting β-lactam cidality by keeping peptidoglycan degradation at bay. Consistent with the diverse roles for these enzymes in peptidoglycan homeostasis (Dik et al., 2017), the prolonged, post-CuAAC recovery in liquid medium of synthetically cross-linked *E. coli* (Figures S6D-E) may also

reflect slowed cell wall turnover. Treatment with unnatural D-amino acids alone modestly enhanced both lag phase and β-lactam tolerance (Figure S6D, S6E, S8), although the effects were not statistically significant. As noncanonical D-amino acid incorporation is not expected to alter cell wall turnover by lytic transglycosylases (Caparros et al., 1992), we speculate that these more-subtle peptidoglycan modifications impact *E. coli* physiology by a different mechanism(s) than the synthetic cross-links.

Given the promiscuity with which D-amino acids incorporate into the bacterial peptidoglycan (Radkov et al., 2018; Siegrist et al., 2015) stapling can be readily adapted for a wide variety of species. Molecular control of synthetic cross-link positioning may also be possible. The effect(s) of 5-5 cross-links on cell wall structure may be different from native, 4,3 or 3,3 cross-links. For example, 5,5 cross-links likely allow more flexibility and/or more space between glycan strands, which could in turn change the physical properties of the peptidoglycan. Unlike monopeptides, which can incorporate into the 4^{th} or 5^{th} positions (or both) of stem peptides (Kuru et al., 2012; Siegrist et al., 2013), D-amino acid dipeptides with functional groups on their N- or C-terminus are predicted to install these groups specifically at 4^{th} or 5^{th} position, respectively (Liechti et al., 2013). Our loss-of-fluorescence assay suggests that dipeptides functionalized with N-terminal azides and alkynes permit the introduction of synthetic, 4-4 cross-links into CS802-2 *E. coli* (Figure S9), in addition to the 5-5 linkages afforded by monopeptide labeling. The development of alkyne- and azide-bearing DAP derivatives may also enable the introduction of triazole linkages at the 3^{rd} position of the muropeptide. Finally, pulse-chase labeling in species with defined modes of growth can offer sub-cellular

control of synthetic cross-links. Independent from and complementary to genetics, cell wall stapling is an orthogonal assay for dissecting the roles of peptidoglycan structure in bacterial physiology.

Significance

Bacteria are surrounded by cell wall heteropolymers that are essential for viability under most circumstances. The structure of the cell wall is well-conserved and consists of a glycan backbone cross-linked by D-amino acid-containing peptides. Cross-link-inhibiting β-lactams account for two-thirds of the global antibiotic market, underscoring the general importance of these linkages to bacterial physiology. For a given species, the density of cross-linking can vary with replication rate and environmental conditions. These changes in cell wall connectivity in turn correlate with other phenotypic properties of the bacterium. However most species have multiple, closely-related enzymes that catalyze cross-links, each with varying susceptibility to different β-lactams, making it difficult to control the density of these linkages by genetics or small molecule inhibition alone. In this work, we present a chemical technique to introduce synthetic cross-links to the cell walls of live bacteria. We use bio-compatible click chemistry to induce a reaction between azido- and alkynyl-D-alanine residues that are metabolically incorporated in the cell wall peptides of Gram-positive and Gram-negative species. The resulting triazole linkages can be visualized by substituting azido-D-alanine with azidocoumarin-D-alanine, an amino acid analogue that becomes more fluorescent after reacting with an alkyne. Stapling the cell wall of *Escherichia coli* enhances its tolerance to β-lactams. Chemical manipulation complements genetic and small molecule

perturbations as an independent means of investigating the role of cell wall connectivity in bacterial physiology.

Acknowledgments

No competing financial interests have been declared. This work was supported by NSF RAISE Convergence 1848065 (M.S.S. under “Palmore”), NSF GRFP (A.K.A.), Stanford ChEM-H Chemistry/Biology Interface Predoctoral Training Program (A.K.A.), American Cancer Society Postdoctoral fellowship PF-18-011-01-CDD (P.S.), NIH R25 GM086264 (C.M.-M.) as well as the Swedish Research Council (VR), Knut and Alice Wallenberg Foundation, Laboratory of Molecular Infection Medicine Sweden (MIMS) and Kempe Foundation (F.C.). We gratefully acknowledge K. Young for *E. coli* strain CS802-2, C. Hill for *pbp5*::tn (*lmo2754*::tn) EGD-e *L. monocytogenes*, and A. Burnside for technical assistance.

Authors Contributions

Conceptualization M.S.S., F.C., S.L.R, A.E., A.K.A.; Investigation, S.L.R., A.E., A.K.A., P.S., C.M.-M. and J.K.; Writing - Original Draft, M.S.S. and S.L.R.; Writing - Review & Editing M.S.S., S.L.R., A.E., and F.C.; Visualization S.L.R.; Funding Acquisition, M.S.S., A.K.A., P.S., F.C.; Supervision, M.S.S., F.C.

Declaration of Interest

The authors declare no competing interests.

Main figure titles and legends

Figure 1. Native (A) and synthetic (B) cross-linking of the bacterial cell wall. Native cross-links are catalyzed by transpeptidases**.** Synthetic cross-links are introduced by metabolic labeling with azido- and alkynyl-D-alanine (azDA and alkDA, respectively) followed by CuAAC.

Figure 2. Loss (A-E) and gain (F and G) of fluorescence strategies for detection of synthetic cross-links. (A) Loss-of-fluorescence logic, including SPAAC control (details in SI Methods). (B-E) *pbp5::tn L. monocytogenes* was incubated with the indicated D-amino acids, washed and subjected to CuAAC with TBTA ligand and alkyne-carboxyrhodamine 110 (CR110) (B); TBTA ligand with azido-CR110 (C); BTTP ligand with alkyne-CR110 (D); SPAAC with DBCO-CR110 (E). Fluorescence was quantified by flow cytometry and data are representative of 2-6 biological replicates performed in triplicate. MFI, mean fluorescence intensity. Error bars, +/- standard deviation. (F), Intra-peptidoglycan reaction between alkDA and azidocoumarin-D-alanine (azcDA) results in the fluorescent triazole product. (G) *pbp5::tn L. monocytogenes* was incubated in the presence of indicated D-amino acids, washed and subjected to BTTP CuAAC with no exogenous fluorescent label. Of the 327 alkDA/azcDA-treated, CuAAC-subjected cells observed in two independent experiments, 310 were fluorescent above Dala/azcDA-treated, CuAAC-subjected background levels. PG, fluorescence derived from peptidoglycan labeling. Scale bar, 1 μM. Images are representative of 4 biological replicates.

Figure 3. Indirect (A-B) and direct (C-E) identification of synthetic triazole cross-links. CS802-2 *E. coli* was incubated +/- D-alanine alone (Dala) or equimolar combinations of D-alanine, azido-D-alanine (azDA), and alkynyl-D-alanine (alkDA) as indicated, washed and subjected to CuAAC with BTTP ligand and complementary fluorophore (A-B) or with the detection reagent omitted (C-E). Peptidoglycan was extracted, digested with mutanolysin and lysozyme, and separated by ultra-performance liquid chromatography (UPLC). We identified several peaks from alkDA/azDA-labeled bacteria that were specific to CuAAC treatment (red and blue boxes, (C)). Chemical structure for 5-5 triazole dimer (D) identified by mass spectrometry (MS) from red boxed peak in (C). (E) Ion detection (left) and MS profile (right) for 5-5 triazole dimer. MS/MS profile and fragmentation shown in Figure S4 and Table S1, respectively. Ion detection and MS profiles for 5-5 triazole trimers and tetramer from blue boxed peaks in (C) shown in Figure S5. Fluorescence in (A-B) was quantified by flow cytometry and data are representative of 2-6 biological replicates performed in triplicate. MFI, mean fluorescence intensity. Error bars, +/- standard deviation. UPLC analysis in (C) was performed on two biological replicates.

Figure 4. Synthetic cross-links protect CS802-2 *E. coli* from ampicillin (B) but not from kanamycin (C). CS802-2 *E. coli* was incubated +/- the indicated D-amino acids for 6 hrs, washed and subjected (B, C) or not (A) to CuAAC with BTTP ligand (no complementary fluorophore) as in Figure 3. Bacteria were then challenged with antibiotic for 1 hr at 37 °C and plated for colony forming units (CFUs). Data are from three biological replicates performed in triplicate. Error bars, +/- standard deviation. Statistical significance was assessed by two-way ANOVA with Tukey's multiple comparison test. ns, ≥ 0.05; *, $p<0.05$; **, $p<0.005$.

Main tables/schemes and legends

Scheme 1. 3-Azido-7-hydroxycoumarin D-alanine synthesis.

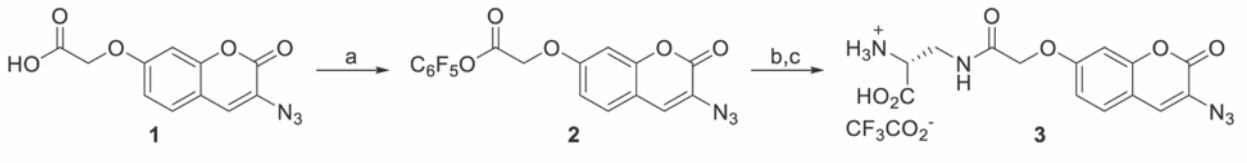

[a]Conditions: (a) Pentafluorophenyl trifluoroacetate, N,N-diisopropylethylamine, THF, rt, 45%. (b) Nα-Boc-D-2,3-diaminopropionic acid, N,N-diisopropylethylamine, 4:1 THF:DMF, 67%. (c) 1:1 TFA:dichloromethane, rt, 79%.

Table 1. Quantification of muropeptides from CS802-2 *E. coli* treated with Dala or a combination of alkDA/azDA then subjected or not to CuAAC.

	Dala		alkDA/azDA	
	-CuAAC	+CuAAC	-CuAAC	+CuAAC
azDA	-	-	8.21 ± 4.26	2.92 ± 0.11
alkDA	-	-	4.04 ± 2.38	1.23 ± 1.32
% PG Modification	-	-	12.24 ± 1.42	11.44 ± 3.39
% Cross-linkage	53.05 ± 2.04	54.31 ± 3.33	42.76 ± 1.57	51.04 ± 0.23
% Triazole Cross-linkage	-	-	-	9.98 ± 1.42

[b]Data from two biological replicates. One of the alkDA/azDA UPLC traces is shown in Figure 3C. Compare to data for bacteria treated with Dala/alkDA or Dala/azDA, Table S2.

417

418 **STAR * Methods**

419 **KEY RESOURCES TABLE**

REAGENT or RESOURCE	SOURCE	IDENTIFIER
Bacterial and Virus Strains		
L. monocytogenes EGDe	Siegrist et. al, 2013	N/A
L. monocytogenes EGDe *pbp5*::tn (*lmo2754*:tn)	Siegrist et. al, 2013	N/A
CS802-2 *E. coli*	Demone et. al, 1999	N/A
Chemicals, Peptides, and Recombinant Proteins		
D-alanine (Dala)	Sigma-Aldrich	Cat# A7377
(R)-α-Propargylglycic (alkDA)	Acros Organics	Cat# 441221000
3-Azido-D-alanine HCl (azDA)	Jena Bioscience	Cat# CLK-AA004
azDlys	Jena Bioscience	
Azido-Coumarin-D-alanine (azcDA)	This paper	N/A
azDADA (ADADA)	Liechti et. al, 2013	https://www.einstein.yu.edu/research/shared-facilities/chemical-biology/
alkDADA (EDADA)	Liechti et. al, 2013	https://www.einstein.yu.edu/research/shared-facilities/chemical-biology/
BTTP	Chemical Synthesis Core Facility, Albert Einstein College of Medicine, Bronx, NY	https://www.einstein.yu.edu/research/shared-facilities/chemical-biology/
TBTA	Click Chemistry Tools, Scottsdale, AZ	Cat# 1061
Copper (II) Sulfate, Anhydrous	Alfa Aesar	Cat# 33308
L-Ascorbic Acid Sodium Salt	Alfa Aesar	Cat# A17759
Carboxyrhodamine 110 Azide (Azide-CR110)	Click Chemistry Tools, Scottsdale, AZ	Cat# AZ105

Carboxyrhodamine 110 Alkyne (Alkyne-CR110)	Click Chemistry Tools, Scottsdale, AZ	Cat# TA106
Carboxyrhodamine 110 DBCO (DBCO-CR110)	Click Chemistry Tools, Scottsdale, AZ	Cat# A127
AFDye 488 Picolyl Azide	Click Chemistry Tools, Scottsdale, AZ	Cat# 1276
Ampicillin Sodium Salt	Fisher Scientific	Cat# BP1760
Kanamycin	Sigma-Aldrich	Cat# K1377
Carbenicillin Disodium Salt	Sigma-Aldrich	Cat# C3416
dichloromethane	Fisher Scientific	
tetrahydrofuran	Fisher Scientific	
N,*N*-dimethylformamide	Fisher Scientific	
N^{α}-Boc-D-2,3-diaminopropionic acid	Chem-Impex International, Inc	
potassium carbonate	Fisher Scientific	
N,*N*-diisopropylethylamine	Acros Organics	
trifluoroacetic acid	Sigma-Aldrich	
Software and Algorithms		
ImageJ	Schneider et al., 2012	https://imagej.nih.gov/ij/
GraphPad Prism 8.4.0	GraphPad	https://www.graphpad.com/scientific-software/prism/
ChemDraw 18.1	PerkinElmer Informatics	https://www.perkinelmer.com/es/category/chemdraw

RESOURCES AVAILABILITY

Lead Contact

Further information and requests for resources and reagents should be directed to Lead Contact, M. Sloan Siegrist (siegrist@umass.edu)

Material Availability

All unique/stable reagents generated in this study are available from the Lead Contact.

Data and Code Availability

Unpublished custom code, software, or algorithm were not used on this publication.

METHODS DETAILS

Culture conditions

E. coli was grown in Luria-Bertani Broth (LB) at 37 ºC. *L. monocytogenes* was grown in Brain Heart Infusion Broth (BHI) at 37 ºC.

Metabolic labeling and CuAAC

E. coli were grown overnight at 37 ºC. The next day cultures were back-diluted between 1:50 and 1:500 and D-amino acids (1.25 mM total per sample for monopeptides and 2.5 mM per sample for dipeptides) were added directly in the LB medium. Cells were grown until log phase (OD_{600} 0.6-0.8) then centrifuged for 5 min at 5,000 x g at room temperature (RT). They were then washed with sterile-filtered PBS and subjected to BTTP CuAAC (200 µM $CuSO_4$, 800 µM BTTP [Chemical Synthesis Core Facility, Albert Einstein College of Medicine, Bronx, NY], 2.5 mM sodium ascorbate (freshly prepared), with or without 25 µM of azido or alkynyl fluorescent dye as appropriate) or TBTA CuAAC (1 mM $CuSO_4$, 128 µM TBTA [Click Chemistry Tools, Scottsdale, AZ], 1.2 mM

sodium ascorbate (freshly prepared), with or without 25 μM of azido or alkynyl fluorescent dye [Click Chemistry Tools]) for 1 hr at room temperature, shaking. Samples were then centrifuged, washed thrice with PBS, and either fixed with 2% (v/v) formaldehyde or used in assays described below.

L. monocytogenes were grown overnight at 37 ºC with the D-amino acids (2.5 mM total per sample) then centrifuged for 5 min at 5,000xg at RT. They were washed with PBS and subjected to CuAAC as described for *E. coli*.

General fluorescence analysis

Mean fluorescence intensities (MFI) of bacterial cell populations were obtained by flow cytometry from a BD DUAL LSRFortessa instrument.

Samples were imaged on an inverted Nikon Eclipse Ti microscope equipped with a Hamamatsu Orca Flash 4.0 camera and reconstructed with NIS Elements.

Peptidoglycan composition analysis

200 mL cultures of log-phase CS802-2 *E. coli* were treated with D-amino acids and subjected to BTTP CuAAC as describe above. Bacteria were centrifuged for 5 minutes at 5,000 x g at RT, wash twice with MilliQ water, resuspended in 1 mL MilliQ water then added drop-wise into 80 mL of boiling 4% SDS. Samples were vigorously stirred for 1.5 hr then cooled to RT. The insoluble fraction (PG) was pelleted at 400,000 x g, 15 min, 30 ºC (TLA-100.3 rotor; OptimaTM Max ultracentrifuge, Beckman). SDS was washed

out and the PG was resuspended in 200 µl of 50 mM sodium phosphate buffer pH 4.9 and digested overnight with 30 µg/mL muramidase (Cellosyl). Samples were incubated at 37 °C. PG digestion was stopped by 5 min incubation in a boiling water bath. Coagulated protein was removed by centrifugation. The supernatants were mixed with 150 µL 0.5 M sodium borate pH 9.5, and subjected to reduction of muramic acid residues into muramitol by sodium borohydride treatment (10 mg/mL final concentration, 30 min at RT). Samples was adjusted to pH 3.5 with phosphoric acid. Chromatographic analyses of muropeptides were performed on AQUITY Ultra Performance Liquid Chromatography (UPLC) BEH C18 column (130 Å, 1.7 µm, 2.1 mm by 150 mm; Waters), and peptides were detected at Abs. 204 nm using ACQUITY UPLC UV-Visible Detector. Muropeptides were separated using a linear gradient from buffer A (0.1% of Formic acid in water) to buffer B (0.1% of Formic acid in acetonitrile) in 218 min, and flow 0.25 mL/min. Muropeptide identity was confirmed by MS/MS analysis, using a Xevo G2-XS QTof system (Waters Corporation, USA). Quantification of muropeptides was based on their relative abundances (relative area of the corresponding peak). Cross-linking was determined by the following formula; crosslinking=dimmer+(trimmer/2).

Antibiotic challenge

CS802-2 *E. coli* that had been pre-labeled with D-amino acids for 6 hrs (OD_{600} 0.6) or overnight and subjected or not to BTTP CuAAC were washed with PBS and resuspended in LB medium to a normalized OD_{600} of 0.3 with or without 125 µg/mL ampicillin, 125 µg/mL carbenicillin, or 6.25 µg/mL kanamycin. After 1-5 hrs incubation at

37 ºC, bacteria were washed twice with PBS and plated as 10-fold serial dilutions on LB agar.

Chemical Synthesis and Characterization

Synthesis of azidocoumarin-D-alanine (azcDA)

General Procedures. Reactions were performed in round bottom flasks fitted with rubber septa under a positive pressure of nitrogen. Gas-tight syringes with stainless steel needles or cannulae were used to transfer air- and moisture-sensitive liquids. Flash column chromatography was performed as described by Still *et al*. using granular silica gel (60-Å pore size, 40–63 μm, 4–6% H_2O content, Silicycle)(Still et al., 1978). Analytical thin layer chromatography (TLC) was performed using glass plates pre-coated with 0.25 mm 230–400 mesh silica gel impregnated with a fluorescent indicator (254 nm). TLC plates were visualized by short wave ultraviolet light (254 nm). Concentration of solutions under reduced pressure were carried out on rotary evaporators capable of achieving a minimum pressure of ~2 torr at 29–30 °C unless noted otherwise.

Dichloromethane, tetrahydrofuran, and *N*,*N*-dimethylformamide were were purified by the method of Grubbs *et al*. under a positive pressure of nitrogen(Pangborn et al., 1996).

Instrumentation. Proton nuclear magnetic resonance (^{1}H NMR) spectra were recorded with a Bruker Avance III 500 MHz spectrometer, are reported in parts per million, and

are referenced to the residual protium in the NMR solvent ($CDCl_3$: δ 7.24 ($CHCl_3$), CD_3OD: δ 3.31 (CHD_2OD), DMSO-d_6: δ 2.50 (DMSO-d_5)). Data are reported as follows: chemical shift [multiplicity (s = singlet, d = doublet, t = triplet, sp = septet, m = multiplet), coupling constant(s) in Hertz, integration]. Carbon-13 nuclear magnetic resonance (^{13}C NMR) spectra were recorded with a Bruker Avance III 500 MHz spectrometer, are reported in parts per million, and are referenced from the carbon resonances of the solvent ($CDCl_3$: δ 77.23, CD_3OD: δ 49.15, DMSO-d_6: δ 39.51). Data are reported as follows: chemical shift. Infrared data (IR) were obtained with a Cary 630 Fourier transform infrared spectrometer equipped with a diamond ATR objective and are reported as follows: frequency of absorption (cm^{-1}), intensity of absorption (s = strong, m = medium, w = weak, br = broad). Optical rotations were measured on a P-2000 JASCO polarimeter and compound concentrations are expressed in units of g/100 mL. High resolution mass spectra (HRMS) were recorded by the Harvard University Small Molecule Mass Spectrometry facility on an Agilent 6210 time-of-flight LCMS using an electrospray ionization (ESI) source.

Overall synthetic scheme.

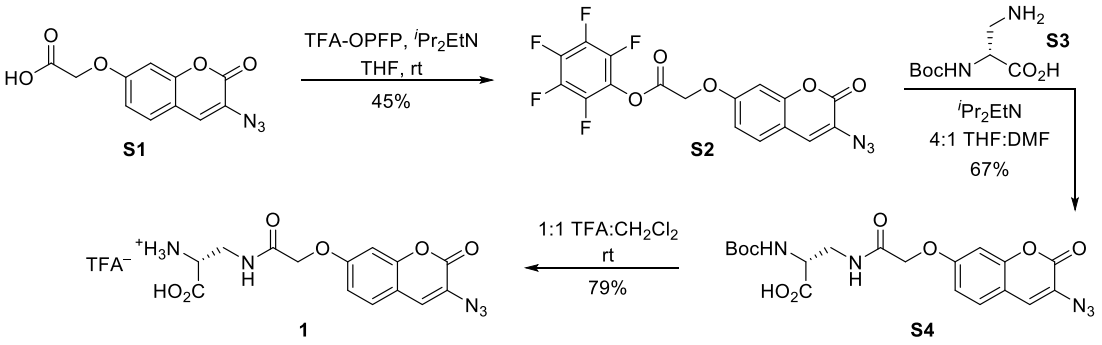

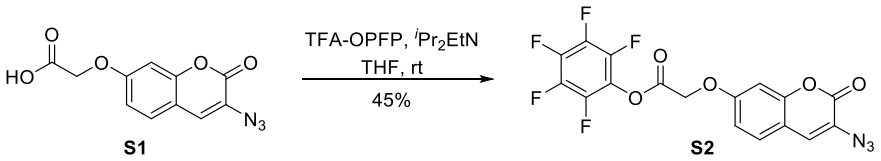

Azidocoumarin pentafluorophenyl ester S3

To a 25 mL round bottom flask charged with azidocoumarin acid **S1**(Weineisen et al., 2017) (56.0 mg, 214 µmol, 1 equiv) under a nitrogen atmosphere was added tetrahydrofuran (2 mL) at room temperature. *N*,*N*-diisopropylethylamine (74.5 µL, 428 µmol, 2.00 equiv) was added to the dark brown solution via syringe. This was followed immediately by addition of pentafluorophenyl trifluoroacetate (73.5 µL, 428 µmol, 2.00 equiv) via syringe and stirred at room temperature. After 30 min, the reaction mixture was concentrated under reduced pressure and the brown residue was purified by flash column chromatography on silica gel (eluent: 10% ethyl acetate in hexanes) to provide the azidocoumarin pentafluorophenyl ester **S2** (41.0 mg, 45%) as a white solid. ^{1}H NMR (500 MHz, $CDCl_3$, 25 °C): δ 7.37 (d, *J* = 8.6 Hz, 1H), 7.15 (s, 1H), 6.93 (dd, *J* = 8.7, 2.5 Hz, 1H), 6.87 (d, *J* = 2.5 Hz, 1H), 5.04 (s, 2H). ^{13}C NMR (126 MHz, $CDCl_3$, 25 °C): δ 164.5, 159.1, 157.6, 152.9, 142.2, 141.2, 140.2, 139.2, 137.2, 128.7, 125.9, 124.7, 114.3, 113.3, 102.2, 64.8. ^{19}F NMR (471 MHz, $CDCl_3$, 25 °C): δ –152.2 (m), –156.4 (m), –161.3 (m). FTIR (thin film, cm^{-1}): 2128 (s), 1804 (m), 1722 (m), 1618 (m), 1521 (s), 1334 (m), 1118 (m), 1070 (m), 995 (m). HRMS (ESI, m/z): 428.0294 (calculated for $C_{17}H_7F_5N_3O_5$ $[M+H]^+$: 428.0300). TLC (15% ethyl acetate in hexanes, R_f): 0.32 (UV).

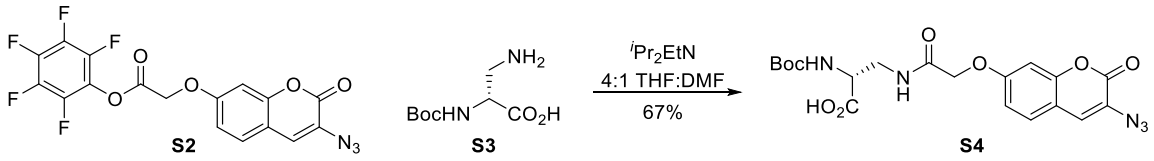

557

558

559 **Boc-D-Ala-azidocoumarin S5**

560 To a 25 mL round bottom flask charged with azidocoumarin pentafluorophenyl ester **S2**
561 (30.0 mg, 70.2 μmol, 1 equiv) and N^{α}-Boc-D-2,3-diaminopropionic acid (**S3**) (28.6 mg,
562 140 μmol, 2.00 equiv) under a nitrogen atmosphere was added tetrahydrofuran (2 mL)
563 at room temperature. *N*,*N*-diisopropylethylamine (14.7 μL, 140 μmol, 2.00 equiv) was
564 then added to the solution via syringe followed by *N*,*N*-dimethylformamide (500 μL).
565 After 20 min, the reaction mixture was concentrated under reduced pressure and the
566 residue was purified by flash column chromatography on silica gel (eluent: 20%
567 hexanes, 75% ethyl acetate, 5% acetic acid) to provide Boc-D-Ala-azidocoumarin **S4**
568 (21.0 mg, 67%) as a white solid. ^{1}H NMR (500 MHz, d_6-DMSO, 25 °C): δ 8.20 (t, J = 6.0
569 Hz, 1H), 7.63 (s, 1H), 7.59 (d, J = 8.5 Hz, 1H), 7.07–6.98 (m, 3H), 4.60 (s, 2H), 4.13–
570 4.05 (m, 1H), 3.57–3.48 (m, 1H), 3.44–3.36 (m, 1H), 1.38 (s, 9H). ^{13}C NMR (126 MHz,
571 d_6-DMSO, 25 °C): δ 172.2, 167.5, 159.7, 157.2, 155.4, 152.4, 128.9, 127.1, 122.6,
572 113.3, 113.1, 101.7, 78.4, 67.2, 53.4, 39.6, 28.2. FTIR (thin film, cm^{-1}): 3366 (br-s),
573 2989 (br-m), 2128 (s), 1737 (m), 1670 (m), 1618 (m), 1521 (m), 1148 (m), 1055 (m).
574 HRMS (ESI, m/z): 446.1324 (calculated for $C_{19}H_{20}N_5O_8$ $[M–H]^-$: 446.1317). TLC
575 (20:75:5 hexanes:ethyl acetate:acetic acid, R_f): 0.18 (UV). $[\alpha]_D^{23}$= +78 (c 0.25, DMSO).

576

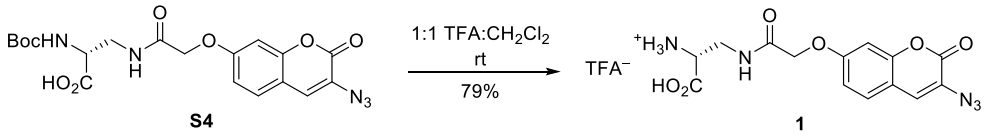

D-Ala-azidocoumarin (1)

To a 25 mL round bottom flask charged with Boc-D-Ala-azidocoumarin **S4** (18.0 mg, 40.2 μmol, 1 equiv) was added dichloromethane (2 mL) followed by trifluoroacetic acid (2 mL) at room temperature. After stirring for 15 min, the reaction mixture was concentrated under reduced pressure and the residue was purified by automated C_{18} reverse phase column chromatography (30 g C_{18} silica gel, 25 μm spherical particles, eluent: H_2O+0.1% TFA (5 CV), gradient 0→100% MeCN/H_2O+0.1% TFA (15 CV), t_R=10.1 CV) to provide the trifluoroacetic acid salt of D-Ala-azidocoumarin (**1**) (11.0 mg, 79%) as a white solid. ^{1}H NMR (500 MHz, d_6-DMSO, 25 °C): δ 8.46 (t, J = 6.0 Hz, 1H), 8.37 (br-s, 3H), 7.64 (s, 1H), 7.59 (d, J = 8.7 Hz, 1H), 7.07 (d, J = 2.2 Hz, 1H), 7.02 (dd, J = 8.6, 2.4 Hz, 1H), 4.63 (s, 2H), 4.06–4.02 (m, 1H), 3.71–3.65 (m, 1H), 3.62–3.56 (m, 1H). ^{13}C NMR (126 MHz, d_6-DMSO, 25 °C): δ 169.2, 168.3, 159.7, 157.2, 152.4, 128.9, 127.2, 122.6, 113.4, 113.1, 101.6, 67.1, 52.2, 38.5. ^{19}F NMR (471 MHz, D_2O, 25 °C) δ –75.6. FTIR (thin film, cm^{-1}): 2117 (s), 1707 (m), 1670 (m), 1618 (s), 1536 (m), 1431 (m), 1170 (m), 1141 (s). HRMS (ESI, m/z): 346.0796 (calculated for $C_{14}H_{12}N_5O_6$ $[M–H]^–$: 346.0793). $[\alpha]_D^{23}$= +68 (c 0.23, DMSO).

References

Aubry, C., Goulard, C., Nahori, M.-A., Cayet, N., Decalf, J., Sachse, M., Boneca, I.G., Cossart, P., and Dussurget, O. (2011). OatA, a Peptidoglycan O-Acetyltransferase

Involved in *Listeria monocytogenes* Immune Escape, Is Critical for Virulence. The Journal of Infectious Diseases *204*, 731-740.

Auer, G.K., and Weibel, D.B. (2017). Bacterial Cell Mechanics. Biochemistry *56*, 3710-3724.

Bertrand, R.L. (2019). Lag Phase Is a Dynamic, Organized, Adaptive, and Evolvable Period That Prepares Bacteria for Cell Division. Journal of Bacteriology *201*.

Boneca, I.G., Dussurget, O., Cabanes, D., Nahori, M.-A., Sousa, S., Lecuit, M., Psylinakis, E., Bouriotis, V., Hugot, J.-P., Giovannini, M.*, et al.* (2007). A critical role for peptidoglycan *N*-deacetylation in *Listeria* evasion from the host innate immune system. Proceedings of the National Academy of Sciences *104*, 997.

Caparros, M., Pisabarro, A.G., and de Pedro, M.A. (1992). Effect of D-amino acids on structure and synthesis of peptidoglycan in *Escherichia coli*. Journal of Bacteriology *174*, 5549-5559.

Cava, F., de Pedro, M.A., Lam, H., Davis, B.M., and Waldor, M.K. (2011). Distinct pathways for modification of the bacterial cell wall by non-canonical D-amino acids. The EMBO Journal *30*, 3442-3453.

Cho, H., Uehara, T., and Bernhardt, T.G. (2014). Beta-lactam antibiotics induce a lethal malfunctioning of the bacterial cell wall synthesis machinery. Cell *159*, 1300-1311.

de Pedro, M.A., Quintela, J.C., Höltje, J.V., and Schwarz, H. (1997). Murein segregation in *Escherichia coli*. Journal of Bacteriology *179*, 2823.

Denome, S.A., Elf, P.K., Henderson, T.A., Nelson, D.E., and Young, K.D. (1999). *Escherichia coli* Mutants Lacking All Possible Combinations of Eight Penicillin Binding Proteins: Viability, Characteristics, and Implications for Peptidoglycan Synthesis. Journal of Bacteriology *181*, 3981.

Dik, D.A., Marous, D.R., Fisher, J.F., and Mobashery, S. (2017). Lytic transglycosylases: concinnity in concision of the bacterial cell wall. Critical Reviews in Biochemistry and Molecular Biology *52*, 503-542.

Dik, D.A., Zhang, N., Chen, J.S., Webb, B., and Schultz, P.G. (2020). Semisynthesis of a Bacterium with Non-canonical Cell-Wall Cross-Links. Journal of the American Chemical Society *142*, 10910-10913.

Egan, A.J., Biboy, J., van't Veer, I., Breukink, E., and Vollmer, W. (2015). Activities and regulation of peptidoglycan synthases. Philos Trans R Soc Lond B Biol Sci *370*.

Eng, R.H., Padberg, F.T., Smith, S.M., Tan, E.N., and Cherubin, C.E. (1991).

Bactericidal effects of antibiotics on slowly growing and nongrowing bacteria. Antimicrob Agents Chemother *35*, 1824-1828.

Fridman, O., Goldberg, A., Ronin, I., Shoresh, N., and Balaban, N.Q. (2014). Optimization of lag time underlies antibiotic tolerance in evolved bacterial populations. Nature *513*, 418-421.

Garcia-Heredia, A., Pohane, A.A., Melzer, E.S., Carr, C.R., Fiolek, T.J., Rundell, S.R., Lim, H.C., Wagner, J.C., Morita, Y.S., Swarts, B.M.*, et al.* (2018). Peptidoglycan precursor synthesis along the sidewall of pole-growing mycobacteria. Elife *7*.

Glauner, B., Holtje, J.V., and Schwarz, U. (1988). The composition of the murein of *Escherichia coli*. J Biol Chem *263*, 10088-10095.

Goodell, W., and Tomasz, A. (1980). Alteration of *Escherichia coli* murein during amino acid starvation. Journal of Bacteriology *144*, 1009-1016.

Huang, K.C., Mukhopadhyay, R., Wen, B., Gitai, Z., and Wingreen, N.S. (2008). Cell shape and cell-wall organization in Gram-negative bacteria. Proceedings of the National Academy of Sciences, pnas.0805309105.

Kohlrausch, U., and Höltje, J.V. (1991). Analysis of murein and murein precursors during antibiotic-induced lysis of *Escherichia coli*. Journal of Bacteriology *173*, 3425.

Kuru, E., Hughes, H.V., Brown, P.J., Hall, E., Tekkam, S., Cava, F., de Pedro, M.A., Brun, Y.V., and VanNieuwenhze, M.S. (2012). In Situ probing of newly synthesized peptidoglycan in live bacteria with fluorescent D-amino acids. Angew Chem Int Ed Engl *51*, 12519-12523.

Lam, H., Oh, D.C., Cava, F., Takacs, C.N., Clardy, J., de Pedro, M.A., and Waldor, M.K. (2009). D-amino acids govern stationary phase cell wall remodeling in bacteria. Science *325*, 1552-1555.

Lee, A.J., Wang, S., Meredith, H.R., Zhuang, B., Dai, Z., and You, L. (2018). Robust, linear correlations between growth rates and β-lactam–mediated lysis rates. Proceedings of the National Academy of Sciences *115*, 4069-4074.

Lee, M., Hesek, D., Llarrull, L.I., Lastochkin, E., Pi, H., Boggess, B., and Mobashery, S. (2013). Reactions of All *Escherichia coli* Lytic Transglycosylases with Bacterial Cell Wall. Journal of the American Chemical Society *135*, 3311-3314.

Lee, S.W., Foley, E.J., and Epstein, J.A. (1944). Mode of Action of Penicillin. Journal of Bacteriology *48*, 393.

Liechti, G.W., Kuru, E., Hall, E., Kalinda, A., Brun, Y.V., VanNieuwenhze, M., and Maurelli, A.T. (2013). A new metabolic cell-wall labelling method reveals peptidoglycan in *Chlamydia trachomatis*. Nature *506*, 507.

Loskill, P., Pereira, P.M., Jung, P., Bischoff, M., Herrmann, M., Pinho, M.G., and Jacobs, K. (2014). Reduction of the Peptidoglycan Crosslinking Causes a Decrease in Stiffness of the *Staphylococcus aureus* Cell Envelope. Biophys J *107*, 1082-1089.

Pangborn, A.B., Giardello, M.A., Grubbs, R.H., Rosen, R.K., and Timmers, F.J. (1996). Safe and Convenient Procedure for Solvent Purification. Organometallics *15*, 1518-1520.

Park, J.T., and Strominger, J.L. (1957). Mode of Action of Penicillin. Science *125*, 99.
Pidgeon, S.E., Fura, J.M., Leon, W., Birabaharan, M., Vezenov, D., and Pires, M.M. (2015). Metabolic Profiling of Bacteria by Unnatural C-terminated D-Amino Acids. Angew Chem Int Ed Engl *54*, 6158-6162.

Pisabarro, A.G., de Pedro, M.A., and Vázquez, D. (1985). Structural modifications in the peptidoglycan of *Escherichia coli* associated with changes in the state of growth of the culture. Journal of Bacteriology *161*, 238.

Radkov, A.D., Hsu, Y.-P., Booher, G., and VanNieuwenhze, M.S. (2018). Imaging Bacterial Cell Wall Biosynthesis. Annual Review of Biochemistry *87*, 991-1014.

Rae, C.S., Geissler, A., Adamson, P.C., and Portnoy, D.A. (2011). Mutations of the *Listeria monocytogenes* Peptidoglycan *N*-Deacetylase and *O*-Acetylase Result in Enhanced Lysozyme Sensitivity, Bacteriolysis, and Hyperinduction of Innate Immune Pathways. Infection and Immunity *79*, 3596.

Scheurwater, E.M., and Burrows, L.L. (2011). Maintaining network security: how macromolecular structures cross the peptidoglycan layer. FEMS Microbiology Letters *318*, 1-9.

Schwarz, U., Asmus, A., and Frank, H. (1969). Autolytic enzymes and cell division of *Escherichia coli*. J Mol Biol *41*, 419-429.

Siegrist, M.S., Swarts, B.M., Fox, D.M., Lim, S.A., and Bertozzi, C.R. (2015). Illumination of growth, division and secretion by metabolic labeling of the bacterial cell surface. FEMS Microbiology Reviews *39*, 184-202.

Siegrist, M.S., Whiteside, S., Jewett, J.C., Aditham, A., Cava, F., and Bertozzi, C.R. (2013). (D)-amino acid chemical reporters reveal peptidoglycan dynamics of an intracellular pathogen. ACS Chemical Biology *8*, 500-505.

733 Sivakumar, K., Xie, F., Cash, B.M., Long, S., Barnhill, H.N., and Wang, Q. (2004). A
734 fluorogenic 1,3-dipolar cycloaddition reaction of 3-azidocoumarins and acetylenes. Org
735 Lett *6*, 4603-4606.
736
737 Spratt, B.G. (1975). Distinct penicillin binding proteins involved in the division,
738 elongation, and shape of *Escherichia coli* K12. Proceedings of the National Academy of
739 Sciences *72*, 2999.
740
741 Still, W.C., Kahn, M., and Mitra, A. (1978). Rapid chromatographic technique for
742 preparative separations with moderate resolution. The Journal of Organic Chemistry *43*,
743 2923-2925.
744
745 Sycuro, L.K., Pincus, Z., Gutierrez, K.D., Biboy, J., Stern, C.A., Vollmer, W., and
746 Salama, N.R. (2010). Peptidoglycan Crosslinking Relaxation Promotes *Helicobacter*
747 *pylori*'s Helical Shape and Stomach Colonization. Cell *141*, 822-833.
748
749 Tomasz, A., Albino, A., and Zanati, E.V.E. (1970). Multiple Antibiotic Resistance in a
750 Bacterium with Suppressed Autolytic System. Nature *227*, 138-140.
751
752 Tomasz, A., and Waks, S. (1975). Mechanism of action of penicillin: triggering of the
753 pneumococcal autolytic enzyme by inhibitors of cell wall synthesis. Proc Natl Acad Sci
754 U S A *72*, 4162-4166.
755
756 Toumanem, E., Cozens, R., Tosch, W., Zak, O., and Tomasz, A. (1986). The Rate of
757 Killing of *Escherichia coli* by B-Lactam Antibiotics Is Strictly Proportional to the Rate of
758 Bacterial Growth. Journal of General Microbiology *132*, 1297-1304.
759
760 Tuomanen, E., and Cozens, R. (1987). Changes in peptidoglycan composition and
761 penicillin-binding proteins in slowly growing *Escherichia coli.* J Bacteriol *169*, 5308-
762 5310.
763
764 Tuomanen, E., Markiewicz, Z., and Tomasz, A. (1988). Autolysis-resistant
765 peptidoglycan of anomalous composition in amino-acid-starved *Escherichia coli*. Journal
766 of Bacteriology *170*, 1373-1376.
767
768 Vollmer, W., and Bertsche, U. (2008). Murein (peptidoglycan) structure, architecture and
769 biosynthesis in *Escherichia coli*. Biochim Biophys Acta *1778*, 1714-1734.
770
771 Vollmer, W., Blanot, D., and de Pedro, M.A. (2008). Peptidoglycan structure and
772 architecture. FEMS Microbiol Rev *32*, 149-167.
773
774 Vollmer, W., and Seligman, S.J. (2010). Architecture of peptidoglycan: more data and
775 more models. Trends Microbiol *18*, 59-66.
776

Wang, W., Hong, S., Tran, A., Jiang, H., Triano, R., Liu, Y., Chen, X., and Wu, P. (2011). Sulfated ligands for the copper(I)-catalyzed azide-alkyne cycloaddition. Chem Asian J *6*, 2796-2802.

Weineisen, N.L., Hommersom, C.A., Voskuhl, J., Sankaran, S., Depauw, A.M.A., Katsonis, N., Jonkheijm, P., and Cornelissen, J.J.L.M. (2017). Photoresponsive, reversible immobilization of virus particles on supramolecular platforms. Chemical Communications *53*, 1896-1899.

Yang, D.C., Blair, K.M., Taylor, J.A., Petersen, T.W., Sessler, T., Tull, C.M., Leverich, C.K., Collar, A.L., Wyckoff, T.J., Biboy, J.*, et al.* (2019). A Genome-Wide *Helicobacter pylori* Morphology Screen Uncovers a Membrane-Spanning Helical Cell Shape Complex. J Bacteriol *201*.

Yang, M., Jalloh, A.S., Wei, W., Zhao, J., Wu, P., and Chen, P.R. (2014). Biocompatible click chemistry enabled compartment-specific pH measurement inside E. coli. Nat Commun *5*, 4981.

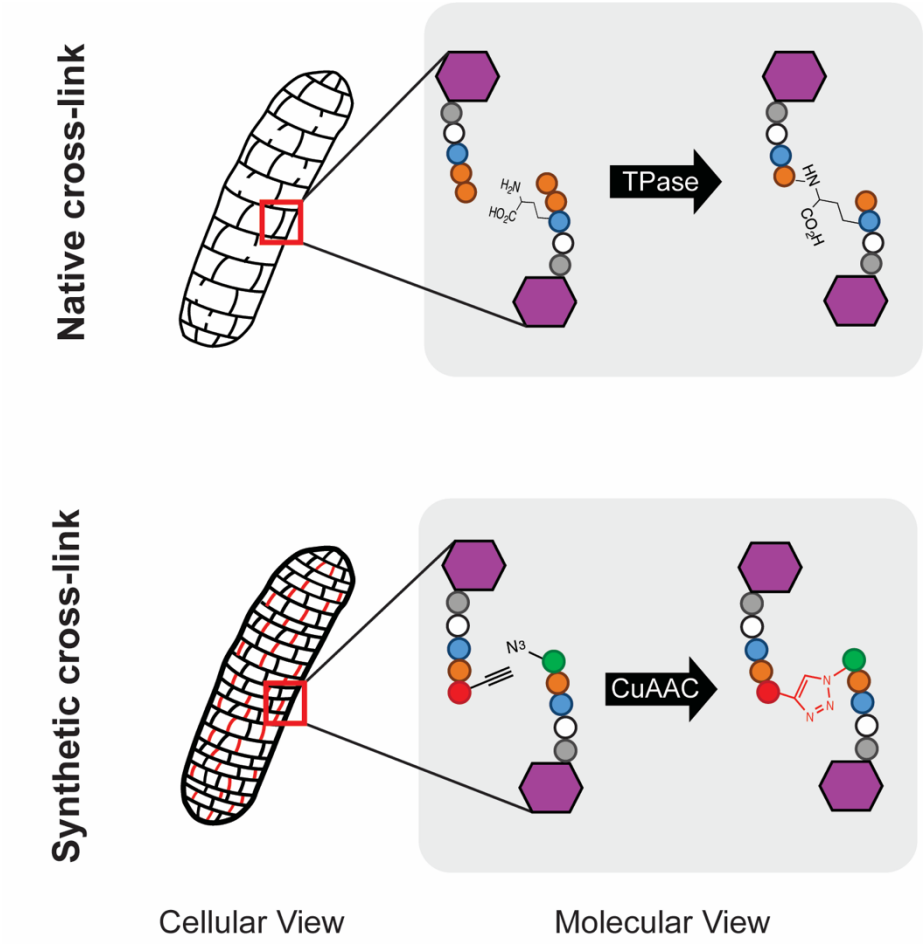

Graphical Abstract

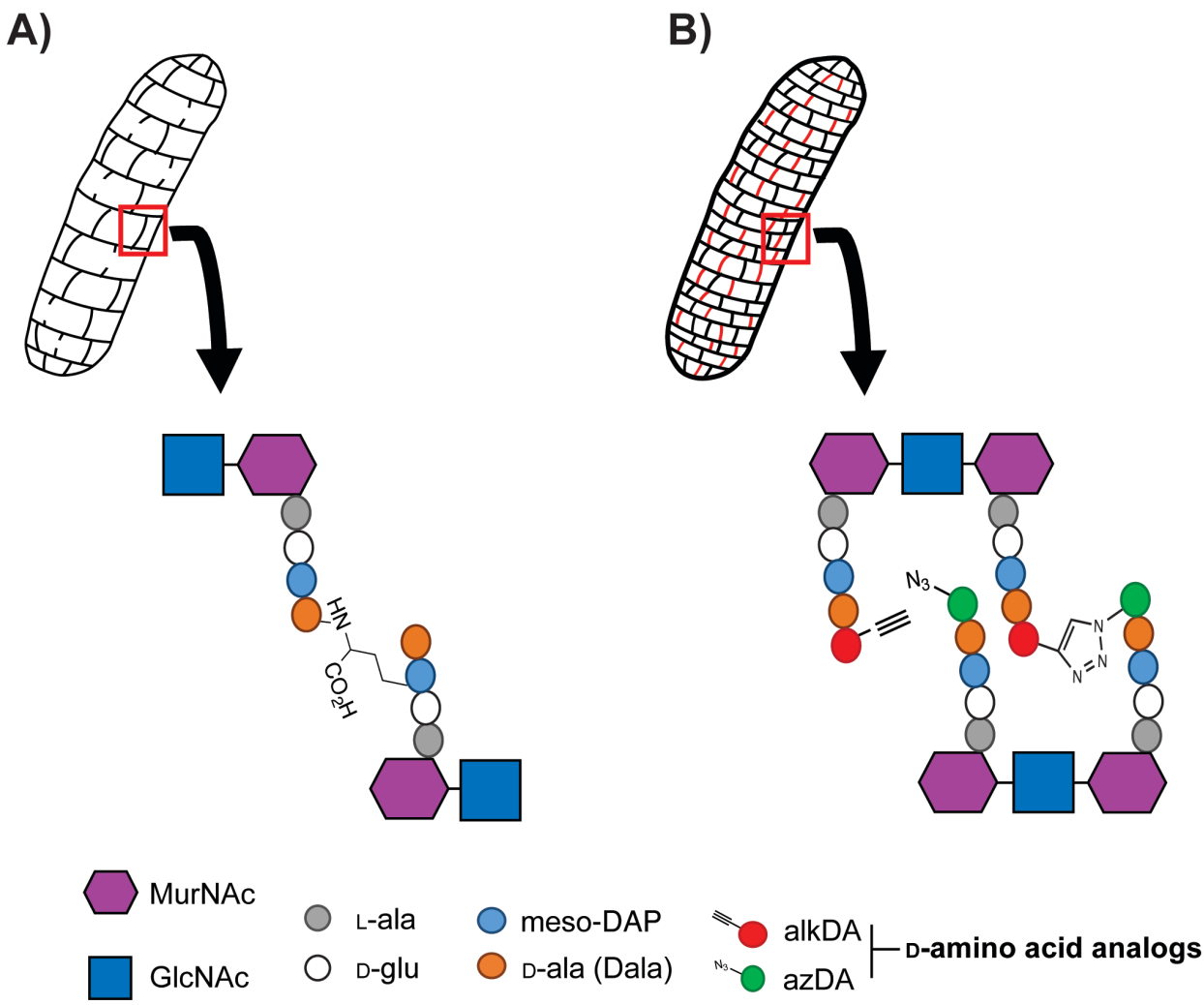

Figure 1. Native (A) and synthetic (B) cross-linking of the bacterial cell wall. Native cross-links are catalyzed by transpeptidases**.** Synthetic cross-links are introduced by metabolic labeling with azido- and alkynyl-D-alanine (azDA and alkDA, respectively) followed by CuAAC.

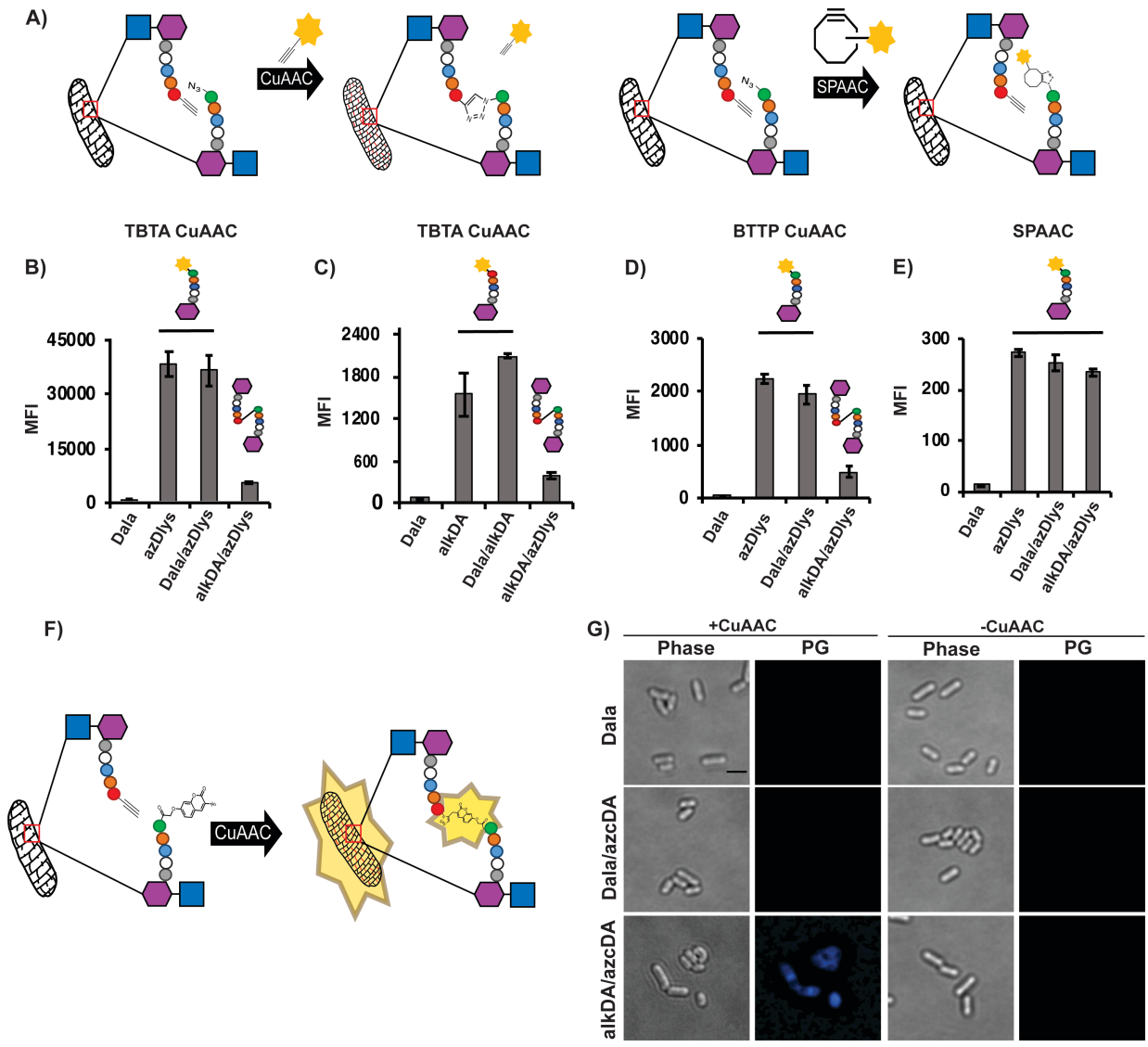

Figure 2. Loss (A-E) and gain (F and G) of fluorescence strategies for detection of synthetic cross-links. (A) Loss-of-fluorescence logic, including SPAAC control (details in SI Methods). (B-E) *pbp5::tn L. monocytogenes* was incubated with the indicated D-amino acids, washed and subjected to CuAAC with TBTA ligand and alkyne-carboxyrhodamine 110 (CR110) (B); TBTA ligand with azido-CR110 (C); BTTP ligand with alkyne-CR110 (D); SPAAC with DBCO-CR110 (E). Fluorescence was quantified by flow cytometry and data are representative of 2-6 biological replicates performed in triplicate. MFI, mean

fluorescence intensity. Error bars, +/- standard deviation. (F), Intra-peptidoglycan reaction between alkDA and azidocoumarin-D-alanine (azcDA) results in the fluorescent triazole product. (G) *pbp5::tn L. monocytogenes* was incubated in the presence of indicated D-amino acids, washed and subjected to BTTP CuAAC with no exogenous fluorescent label. Of the 327 alkDA/azcDA-treated, CuAAC-subjected cells observed in two independent experiments, 310 were fluorescent above Dala/azcDA-treated, CuAAC-subjected background levels. PG, fluorescence derived from peptidoglycan labeling. Scale bar, 1 μM. Images are representative of 4 biological replicates.

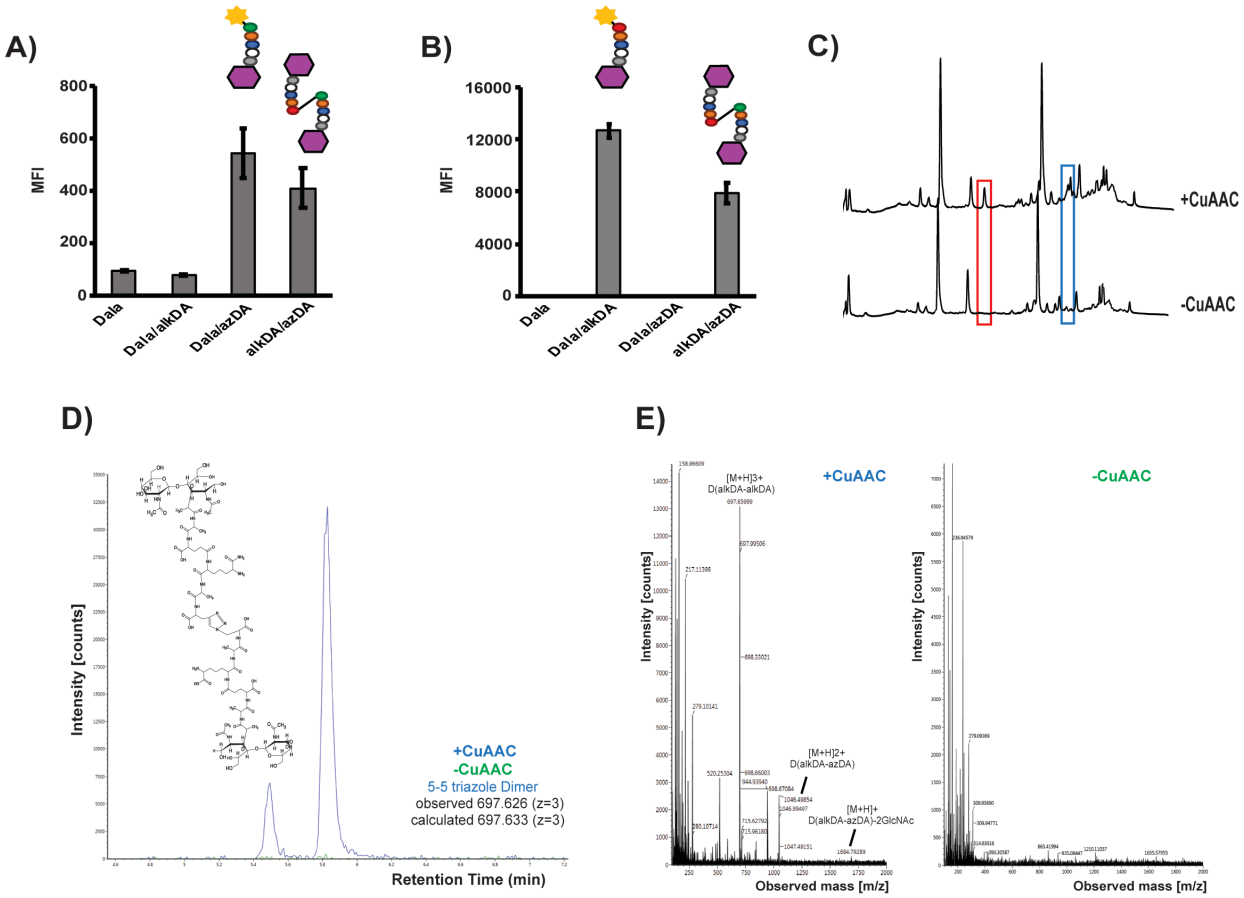

Figure 3. Indirect (A-B) and direct (C-E) identification of synthetic triazole cross-links. CS802-2 *E. coli* was incubated +/- D-alanine alone (Dala) or equimolar combinations of D-alanine, azido-D-alanine (azDA), and alkynyl-D-alanine (alkDA) as indicated, washed and subjected to CuAAC with BTTP ligand and complementary fluorophore (A-B) or with the detection reagent omitted (C-E). Peptidoglycan was extracted, digested with mutanolysin and lysozyme, and separated by ultra-performance liquid chromatography (UPLC). We identified several peaks from alkDA/azDA-labeled bacteria that were specific to CuAAC treatment (red and blue boxes, (C)). Chemical structure for 5-5 triazole dimer (D) identified by mass spectrometry (MS) from red boxed peak in (C). (E) Ion detection (left) and MS profile (right) for 5-5 triazole dimer. MS/MS profile and fragmentation shown

in Figure S4 and Table S1, respectively. Ion detection and MS profiles for 5-5 triazole trimers and tetramer from blue boxed peaks in (C) shown in Figure S5. Fluorescence in (A-B) was quantified by flow cytometry and data are representative of 2-6 biological replicates performed in triplicate. MFI, mean fluorescence intensity. Error bars, +/- standard deviation. UPLC analysis in (C) was performed on two biological replicates.

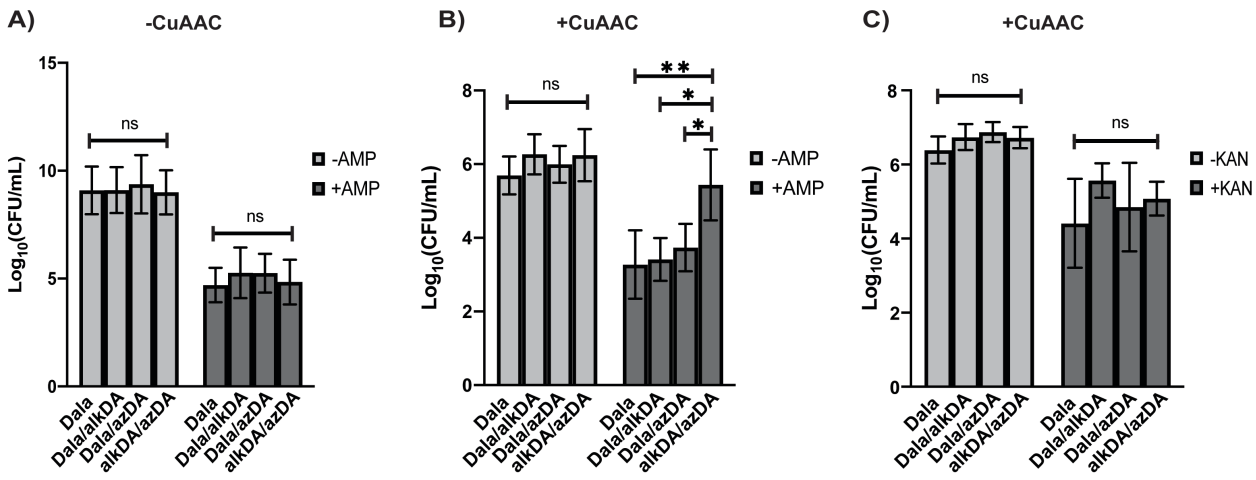

858

859 **Figure 4.** Synthetic cross-links protect CS802-2 *E. coli* from ampicillin (B) but not from
860 kanamycin (C). CS802-2 *E. coli* was incubated +/- the indicated D-amino acids for 6 hrs,
861 washed and subjected (B, C) or not (A) to CuAAC with BTTP ligand (no complementary
862 fluorophore) as in Figure 3. Bacteria were then challenged with antibiotic for 1 hr at 37 °C
863 and plated for colony forming units (CFUs). Data are from three biological replicates
864 performed in triplicate. Error bars, +/- standard deviation. Statistical significance was
865 assessed by two-way ANOVA with Tukey's multiple comparison test. ns, ≥0.05; *, $p<0.05$;
866 **, $p<0.005$.

867

868

869

870

871

872

873

874

Main tables/schemes and legends

Scheme 1. 3-Azido-7-hydroxycoumarin D-alanine synthesis.

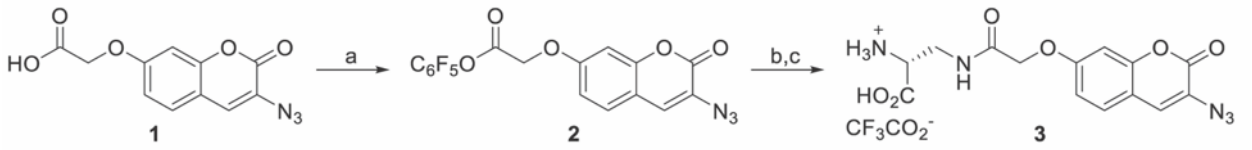

[a]Conditions: (a) Pentafluorophenyl trifluoroacetate, N,N-diisopropylethylamine, THF, rt, 45%. (b) Nα-Boc-D-2,3-diaminopropionic acid, N,N-diisopropylethylamine, 4:1 THF:DMF, 67%. (c) 1:1 TFA:dichloromethane, rt, 79%.

Table 1. Quantification of muropeptides from CS802-2 *E. coli* treated with Dala or a combination of alkDA/azDA then subjected or not to CuAAC.

	Dala		alkDA/azDA	
	-CuAAC	+CuAAC	-CuAAC	+CuAAC
azDA	-	-	8.21 ± 4.26	2.92 ± 0.11
alkDA	-	-	4.04 ± 2.38	1.23 ± 1.32
% PG Modification	-	-	12.24 ± 1.42	11.44 ± 3.39
% Cross-linkage	53.05 ± 2.04	54.31 ± 3.33	42.76 ± 1.57	51.04 ± 0.23
% Triazole Cross-linkage	-	-	-	9.98 ± 1.42

[b]Data are average of two biological replicates. One of the alkDA/azDA UPLC traces is shown in Figure 3C. Compare to data for bacteria treated with Dala/alkDA or Dala/azDA, Table S2.

892
893